

PHOTOLUMINESCENCE INVESTIGATIONS OF InGaAsN
ALLOYS LATTICE-MATCHED TO GaAs

E. D. Jones, N. R. Modine, A. A. Allerman,
I. J. Fritz, S. R. Kurtz, and A. F. Wright
Sandia National Laboratories
Albuquerque, NM 87185, USA

S. T. Tozer and Xing Wei
National High Magnetic Field Laboratory
Tallahassee, FL 32306

RECEIVED
JUN 09 1999
OSTI

InGaAsN is a semiconductor alloy system with the property that the inclusion of only 2% nitrogen reduces the bandgap by more than 30%. In this paper, we have measured the conduction-band mass measurements by three different techniques for 2% nitrogen in InGaAsN lattice matched to GaAs. Additionally, we also report pressure dependent measurements of the conduction-band mass between ambient and 40 kbar. Based on our results, we suggest that the observed changes in masses are a result of Γ -X mixing.

INTRODUCTION

The quaternary alloy system, InGaAsN, is a new material system that appears to have important device applications. Because of a large negative "bowing" parameter,^{1,2} the addition of small amount of nitrogen to the 1.4 eV bandgap energy of the GaAs system drastically lowers the energy! Besides also lowering the bandgap energy, adding indium to GaAsN strain compensates the effect of nitrogen, resulting in a material system with bandgap energies \sim 1eV, lattice matched to GaAs! The InGaAsN, alloy system has been identified as a key candidate material for long wavelength laser systems³⁻⁵ and high-efficiency multi-junction solar cells.^{6,7} Presently, the main questions regarding the role of the nitrogen isoelectronic atom are: (1) What is the origin of the large bandgap reduction? (2) Are the states extended (band-like) or localized (impurity-like)? (3) How is the GaAs conduction-band effective mass $m_c = 0.067$ affected by the addition of nitrogen?

Recently, we have reported a first principles calculation for the electronic bandstructure of InGaAsN.⁸ We found that the large bandgap reduction is due to Γ -L and Γ -X mixing and hence resulting in repulsion between the Γ -L and Γ -X GaAs bands. The pressure dependence of the Γ -like conduction band was calculated for 2% nitrogen in InGaAsN and excellent agreement between theory and experiment was reported.⁸

Thus, items (1) and (2), listed above, have been addressed⁸ with some certainty. Item (3), concerning masses, is the subject of this paper. We have measured of the conduction-band effective mass using three different experimental techniques: (1) Low-temperature bandgap energy as a function of InGaAsN/GaAs quantum-well widths. (2) Photoreflectance measurements of the ground state and excited state energies of InGaAsN/GaAs quantum wells. (3) Magnetoluminescence measurements of the magnetic field dependence of the InGaAsN exciton diamagnetic shift in bulk epilayers. Additionally, the pressure dependence of the conduction-band energy and mass has also been determined from the diamagnetic shift measurements.

DISCLAIMER

This report was prepared as an account of work sponsored by an agency of the United States Government. Neither the United States Government nor any agency thereof, nor any of their employees, make any warranty, express or implied, or assumes any legal liability or responsibility for the accuracy, completeness, or usefulness of any information, apparatus, product, or process disclosed, or represents that its use would not infringe privately owned rights. Reference herein to any specific commercial product, process, or service by trade name, trademark, manufacturer, or otherwise does not necessarily constitute or imply its endorsement, recommendation, or favoring by the United States Government or any agency thereof. The views and opinions of authors expressed herein do not necessarily state or reflect those of the United States Government or any agency thereof.

DISCLAIMER

**Portions of this document may be illegible
in electronic image products. Images are
produced from the best available original
document.**

EXPERIMENTAL

The structures were grown in a vertical flow, high speed rotating disk, EMCORE GS/3200 metalorganic chemical vapor deposition (MOCVD) reactor. The $\text{In}_x\text{Ga}_{1-x}\text{As}_{1-y}\text{N}_y$ films were grown using trimethylindium (TMIn), trimethylgallium (TMG), 100% arsine and dimethylhydrazine (DMHy). Dimethylhydrazine was used as the nitrogen source since it has a lower disassociation temperature than ammonia and has a vapor pressure of approximately 110 torr at 18°C. Unintentionally doped InGaAsN was p-type. InGaAsN films for Hall and optical measurements were grown on semi-insulating GaAs orientated 2° off (100) towards <110>. Lattice matched ($\delta a / a < 8 \times 10^{-4}$) films were grown at 600°C and 60 torr using a V/III ratio of 97, a DMHy/V ratio of 0.97 and a TMIn/III ratio of 0.12. The growth rate was 10 Å/s. These conditions resulted in films with an indium mole fraction of 0.07 ± 0.005 and a nitrogen mole fraction of 0.022 ± 0.003 . The composition was determined by calibration growths of GaAsN and InGaAs along with double crystal x-ray diffraction measurements. The nitrogen composition of bulk films was also confirmed from elastic recoil detection measurements. A significant increase in photoluminescence intensity was observed from these films following a post-growth anneal. Ex-situ, post-growth anneals were carried out in a rapid thermal anneal system under nitrogen using a sacrificial GaAs wafer in close proximity to the InGaAsN sample.

The photoluminescence intensity was a maximum for samples annealed either at 700°C for 2 minutes or at 650°C for 30 minutes. Similar results have been reported by Rao *et.al.*⁹ Transmission electron microscopy measurements indicate that the samples are random and no evidence for clustering or phase separation was observed.¹⁰ The pressure was generated using a small BeCu piston-cylinder diamond anvil cell, 8.75-mm-diameter and 12.5-mm-height.¹¹ Methanol, ethanol, and water in a ratio of 16:3:1 was used for the pressure medium.¹² The shift in the fluorescence of a small chip of ruby placed in the pressurized volume was used to calibrate the pressure at 4K with an accuracy of ± 0.5 kbar.¹³ A single 600-μm-diameter optical fiber, butted up against one of the diamonds, directed the 1 mW power 5145-nm-wavelength laser to the sample and also collected the PL signal from the sample. A beam splitter system was used to direct the PL signal to an optical monochromator. Depending on the bandgap energy, two liquid-nitrogen-cooled detectors were used to detect the PL signal. For low pressure regimes, where the bandgap energies were near or below 1 eV, a NORTH-COAST EO-817L Ge-detector was employed, while at higher pressures, a standard CCD array was used.

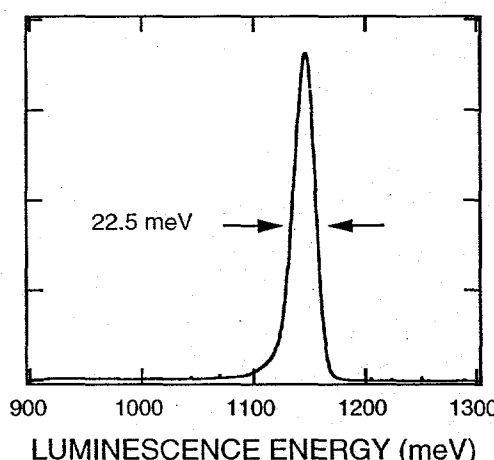


Figure 1. Low temperature (4K) PL spectrum for an annealed InGaAsN sample with 2% N. The FWHM = 22.5 meV. The 4-K bandgap energy of 1150 meV drops to 1050 meV at 300K.

Photoreflectance spectra were obtained for a variety of MOCVD InGaAsN/GaAs quantum well structures. For these experiments, the optical pump source was a blue LED having a 15 degree divergence angle and a peak emission wavelength of 470 nm (Nichia Chemical Industries, part number NSPB 300A.) The LED was driven by a square-wave current source operating at 15 mA and 325 Hz. The sample reflectance was measured using a 10 W tungsten-halogen lamp followed by a 0.25-m grating monochromator in conjunction with an InGaAs photodiode detector and a lock-in amplifier.

DISCUSSION

A typical low temperature (4K) PL spectrum for 2% nitrogen in InGaAsN lattice matched to GaAs is shown in Fig. 1. As can be seen, the 4-K bandgap energy is near 1150 meV, which is significantly less than the 4-K GaAs bandgap energy $E_g \approx 1515$ meV. At room temperature, the bandgap energy is about 1.05 eV. The full-width-half-maximum (FWHM) PL linewidth is about 22.5 meV. As mentioned above, the PL intensity increased significantly with annealing. Other optical parameters, such as the FWHM and PL-peak energy appear to remain unaffected by our annealing process.

Because of low conduction-band mobilities (~ 400 cm²/V-sec), we are unable to perform cyclotron resonance measurements which would have allowed a direct mass determination. Thus we employed three alternate and relatively simple methods of using optical measurements for masses, and they are: (1) Change in luminescence energy in quantum well structures as a function of the quantum-well width. (2) Measuring the electronic quantum well energies by photoreflectance measurements. (3) Analysis of exciton diamagnetic shifts as a function of magnetic field.

A series of nominally 2% nitrogen InGaAsN/GaAs quantum wells were grown as previously described above. The quantum-well widths were estimated from growth rate calibrations. The PL measurements were made at 4K and the resulting dependence of the bandgap energy on the quantum-well width is shown in Fig. 2. The quantum well widths varied between 50 and 200 Å, and as can be seen in Fig. 2, the luminescence energy increases with decreasing quantum well width, the anticipated result. We are interested in comparing the InGaAsN and GaAs masses and thus for purposes of this paper, we will analyze the quantum well data in a simple manner assuming infinite barrier heights. This assumption is probably acceptable because of the large (400 meV) conduction-band offset between InGaAsN and GaAs. Because all of the mass measurements presented here are only to serve as an illustration of the effect of nitrogen in GaAs, we feel that this simple assumptions is warranted. Using the infinite barrier approximation, the luminescence energy for a particle of mass m and quantum-well width A is given by

$$E(n) = \frac{\pi^2 \hbar^2 n^2}{2mA^2} = \frac{37600n^2}{m^* L^2}, \quad [1]$$

where $n = 1, 2, \dots$ is the quantum number of the state, m^* is the conduction-band effective mass in terms of the free electron mass m_0 , and L is the quantum well width in Angstroms. The conduction-band mass and not the reduced mass is used in Eq. (1). The justification for this assumption is that the valence-band offset between 2% nitrogen in InGaAsN and GaAs is believed to be small and only due to the valence-band offset from the 7% indium

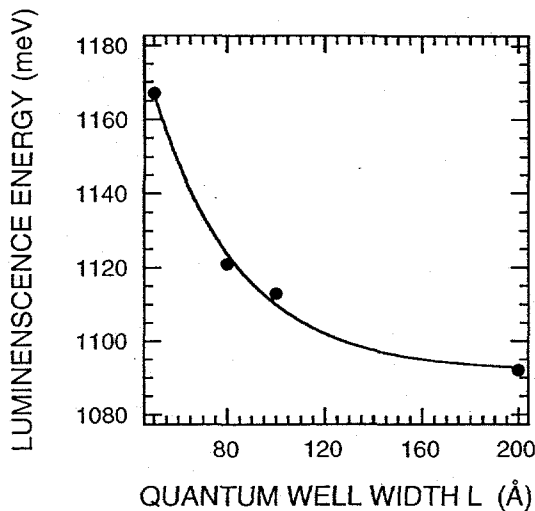


Figure 2. Luminescence energy versus quantum-well width L for single quantum wells of InGaAsN/GaAs at 4K. The smooth curve drawn through the data is provided an aid to the eye.

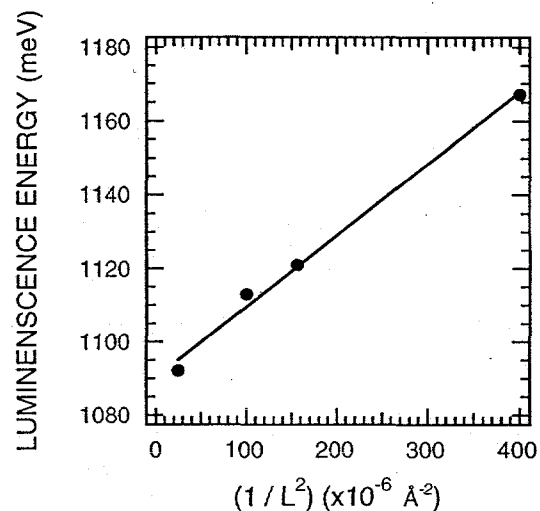


Figure 3. Luminescence energy versus the square of the inverse quantum-well width, i.e., L^{-2} for InGaAsN/GaAs quantum wells at 4K. The straight line fit to the data yields a conduction-band effective mass $m_c \sim 0.2$

content.^{3,4} Thus, we assume that quantum confinement does not result in any large splitting between the “pinned” heavy-hole and light-hole valence bands, thereby leading to a “heavy” valence-band mass. Figure 3 shows the dependence of the luminescence energy as a function of L^{-2} for the data shown in Fig. 2, and as can be seen, a straight line can be drawn through the data. From the slope of the line shown in Fig. 3 and with $n = 1$ (Eq. (1)), we derive $m_c \sim 0.2$. Possible sources of error are the experimental values for quantum-well widths, which are difficult to monitor or control during growth, and possible nitrogen content differences between samples and hence bandgap energy variations. The quantum well samples were grown sequentially in order to minimize nitrogen concentration variations. The conduction-band effective mass for GaAs is $m_c \approx 0.067$ and thus, as in the case of the bandgap energy, we see that the addition of a small amount of nitrogen to GaAs has caused large changes to the 2% nitrogen InGaAsN conduction-band mass.

As a further verification for the apparent heavy conduction-band mass, we have also performed room temperature photoreflectance measurements on the similar structures to those used for the luminescence bandgap energy versus quantum-well-width studies. Figure 4 shows photoreflectance spectra for 50, 80, 100 and 200-Å-wide quantum wells. The solid lines are “fitted” theoretical photoreflectance line shapes to the data. The vertical lines are the critical point energies (i.e., quantum well energies) for each spectrum as calculated by the theoretical line shape fit. The energy difference δE between the 80-Å-wide quantum well states shown in Fig. 4 is $\delta E \sim 120$ meV. We again make the assumption that this energy difference is due only to the conduction-band states. With infinite barrier heights, we can arrive at a qualitative estimate for the conduction-band mass from Eq. (1), with the result $m_c \sim 0.14$, a mass twice as large as that found for GaAs!¹⁴ The two measurement techniques for the mass using InGaAsN/GaAs quantum wells are in reasonable agreement with each other and lead to the conclusion that the conduction-band mass in InGaAsN is two to three times heavier than the GaAs conduction-band mass.

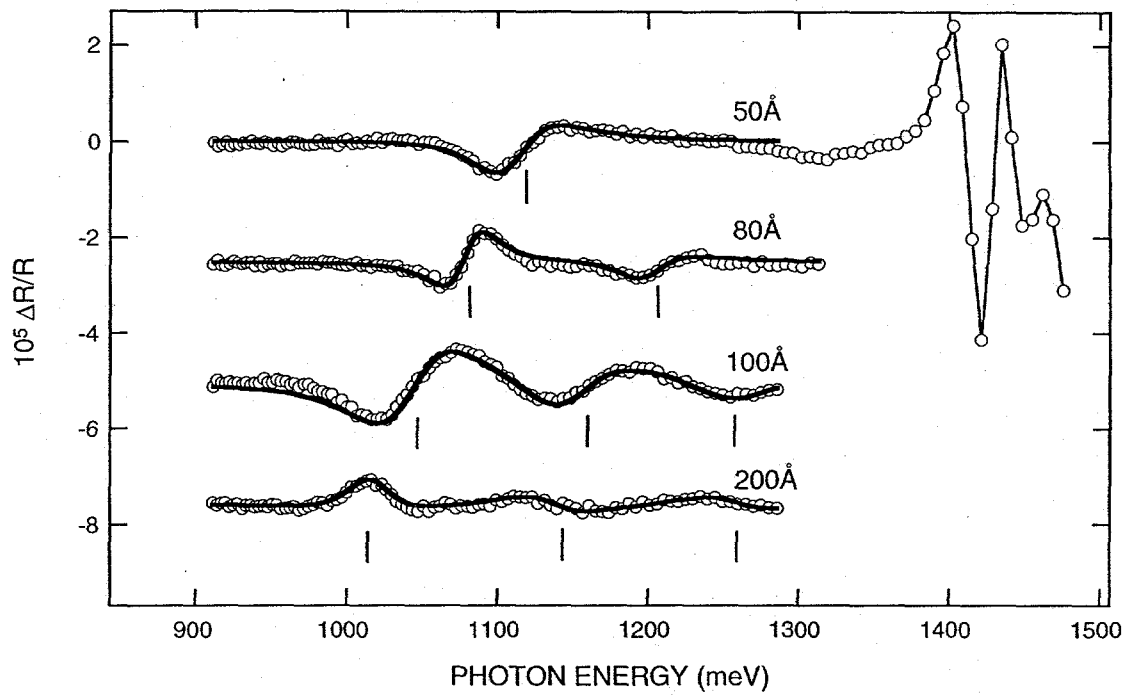


Figure 4. Photoreflectance spectra for four different InGaAsN/GaAs quantum well structures. The quantum-well widths are indicated in the figure. The solid lines are “fitted” theoretical photoreflectance line shapes to the data. The vertical lines are the critical point energies (i.e., quantum well energies) for each spectrum as calculated by the theoretical line shape fit. As an aid to the eye, the spectra have been offset from each other.

The last experimental method for an optical determination of the conduction-band mass involves measurements of the exciton diamagnetic shift as a function of magnetic field for 2% nitrogen InGaAsN alloys lattice matched to GaAs. The magnetoexciton diamagnetic shift dependence on magnetic field for ambient pressure is shown as closed circles in Fig. 5. The diamagnetic shifts for varying InGaAsN conduction-band mass m_c between 0.067 and 0.5 are also indicated in the figure. The theoretical diamagnetic shifts were calculated by the variational approach as described by Greene and Bajaj.^{15,16} The trial wavefunctions for the exciton center-of-mass coordinate system are expressed in terms of a Gaussian basis set. Besides the low temperature bulk GaAs bandgap energy, the magnetic field strength, and the quantum-well width, some of the relevant physical parameters include: (1) The Luttinger parameters γ_1 and γ_2 for both the InGaAsN quantum well and GaAs barriers. (2) Conduction and valence-band mass values for the InGaAsN epilayer. (3) Low frequency dielectric constants ϵ_0 for InGaAsN. For these calculations, GaAs values for all parameters except the conduction-band mass were used. For the present level of understanding the electronic properties of InGaAsN alloys, these assumptions are reasonable. As can be seen in Fig. 3, a best fit diamagnetic shift dependence on magnetic field occurs for an InGaAsN conduction-band effective mass $m_c \approx 0.13$, which is in excellent agreement with the two previous optical determinations described above.

As mentioned in the experimental section, pressure dependent magnetoluminescence measurements were performed in the pressure range of ambient to 110 kbar and magnetic fields up to 30 tesla. The diamagnetic shift data can be readily analyzed for pressures less than 40 kbar. For higher pressures, the accuracy of the technique fails because of linewidth

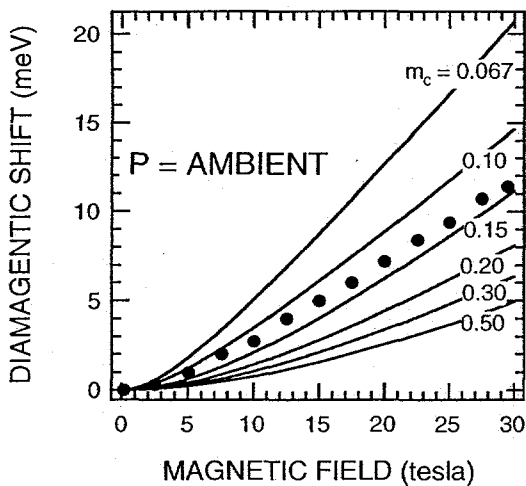


Figure 5. Ambient-pressure exciton diamagnetic shift as a function of magnetic field at 2K for the 2% nitrogen InGaAsN alloy. The closed circles are the experimental points. The curves, labeled $m_c = 0.067$ to 0.50 , are calculated diamagnetic shifts as a function of mass. The estimated ambient pressure InGaAsN conduction-band effective mass m_c is about 0.13 .

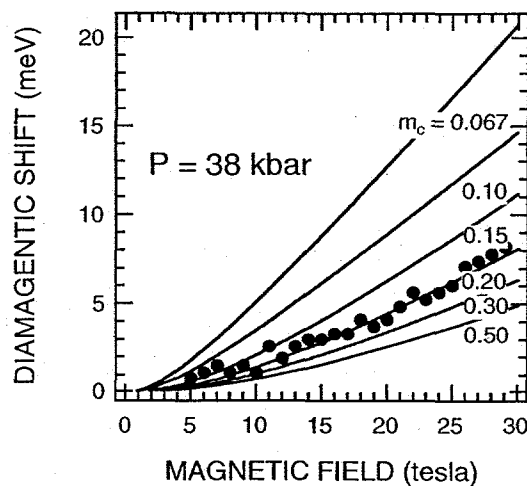


Figure 6. Exciton diamagnetic shift as a function of magnetic field and 38 kbar at 2K for the 2% nitrogen InGaAsN alloy. The closed circles are the experimental points. The curves, $m_c = 0.067$ to 0.50 , are theoretical diamagnetic shifts as a function of mass. The InGaAsN conduction-band effective mass at 38 kbar is $m_c \approx 0.2$.

broadening by the non-hydrostatic component of the pressure medium and also because of a large increase of the conduction-band mass as discussed below. Also, other broadening mechanisms include possible differences to the GaAs elastic constants with the addition of 2% nitrogen. If the elastic constant differences between GaAs substrate and the InGaAsN epilayer are significant, the application of pressure (including hydrostatic pressure) will lead to anisotropic strain in the InGaAsN epilayer and hence large PL linewidths.

Figure 6 shows the magnetic field dependence of the exciton diamagnetic shift at 38 kbar and $T = 2K$. Again the filled circles are the data points and the curves are calculated shifts as a function of mass. It is apparent from the figure that the conduction-band effective mass is nearly 0.2 in contrast to the $m_c \approx 0.13$ found from the ambient pressure data. This large increase to the mass for 2% nitrogen in GaAs is surprising. Recently, mass measurements as a function of pressure in $\text{In}_{0.2}\text{Ga}_{0.8}\text{As}/\text{GaAs}$ strained-single-quantum wells were reported¹⁴ and that the conduction-band mass ranged from ~ 0.07 to ~ 0.085 for pressures between ambient and 36 kbar in a linear manner. This result for InGaAs/GaAs agrees with expectations¹⁴ based on simple $k \cdot p$ theory. The large variation and nonlinear behavior of the conduction-band mass for InGaAsN may not be that surprising in light of all of the other mysteries associated with substituting nitrogen for arsenic in GaAs. Figure 7 shows the variation of the effective mass for pressures between ambient and 38 kbar. The smooth curve provides an aid to the eye.

Because of our success in using the LDA calculation⁸ to quantify the change in the bandgap energy with pressure, we performed preliminary LDA calculations for the pres-

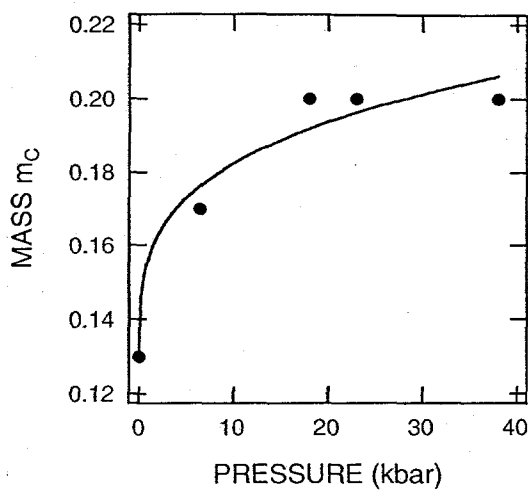


Figure 7. The 2-K pressure dependence of the conduction-band mass between ambient pressure and 40 kbar for the 2% nitrogen InGaAsN sample. The smooth curve drawn through the data provides an aid to the eye.

sure dependence of the conduction-band mass. But to date, our results are inconclusive and hence will not be discussed here. We can, however, make some qualitative statements by examining the LDA results reported in Ref. 8. As discussed in this paper, the band repulsion between the Γ -like and X-like bands at high pressure indicate that strong Γ -X mixing is occurring. The amount of Γ -L and Γ -X mixing is pressure dependent with the contribution from the Γ -L mixing decreasing with pressure and while that from the Γ -X amount is increasing with pressure. Because the mass of the six-fold degenerate X-point in GaAs is heavy ($m_{Xt} = 1.2$ & $m_{XI} = 0.27$), we expect that the Γ -X mixing will cause a corresponding pressure dependent increase to the Γ -like conduction-band mass by the heavy X-like mass. Part of the LDA mass calculation will require information about the X-like as well as the L-like masses. In the future, an obvious goal of our LDA calculations will be to predict the dependence shown in Fig. 6.

CONCLUSIONS

The conduction-band effective mass was measured by three techniques with the result for a 2% InGaAsN alloy, lattice matched to GaAs, the InGaAsN conduction-band effective mass $m_c \approx 0.15$. The pressure dependence of the conduction-band mass is nonlinear and large. The current challenge of the LDA calculation is to account for this behavior.

ACKNOWLEDGEMENTS

Sandia is a multiprogram laboratory operated by Sandia Corporation, a Lockheed Martin Company, for the United States Department of Energy under contract DE-AC04-94AL85000. Part of this work was performed at the National High Magnetic Field Laboratory, which is supported by NSF Cooperative Agreement No. DMR-9016241 and by the State of Florida.

REFERENCES

1. W. G. Bi and C. W. Tu, *Appl. Phys. Lett.* **70**, 1608 (1997).
2. L. Malikova, F. H. Pollak, and R. Bhat, *J. Electronic Materials* **27**, 484 (1998).
3. M. Kondow, K. Uomi, A. Niwa, T. Kitatani, S. Watahiki, and Y. Yazawa, *Jpn. J. Appl. Phys.* **35**, 1273 (1996).
4. M. Kondow, T. Kitatani, S. Nakatsuka, M. C. Larson, K. Nakahara, Y. Yazawa, M. Okai, and K. Uomi, *IEEE J. Selected Topics in Quantum Electronics* **3**, 719 (1997).

5. T. Miyamoto, K. Takeuchi, F. Koyama, and K. Iga, IEEE Photonics Tech. Lett. **9**, 1448 (1997).
6. Sarah R. Kurtz, D. Myers, and J. M. Olsen, in *Proc. 26th IEEE Photovoltaics Spec. Conf.* (IEEE, New York, 1997) pp. 875-878.
7. Steven R. Kurtz, A. A. Allerman, E. D. Jones, J. M. Gee, J. J. Banas, and B. E. Hammons, To be published, *Appl. Phys. Lett.* (1999)
8. E. D. Jones, N. A. Modine, A. A. Allerman, Steven R. Kurtz, A. F. Wright, S. T. Tozer, and X. Wei, To be published, *Phys. Rev. B* (1999).
9. E. V. K. Rao, A. Ougazzaden, Y. Le Bellego, and M. Juhel, *Appl. Phys. Lett.* **72**, 1409 (1998).
10. D. M. Follstaedt (Unpublished results.)
11. S. W. Tozer (Unpublished results.)
12. G. J. Piermarini, S. Block, J. D. Barnett, *J. Appl. Phys.* **44**, 5377 (1973).
13. R. A. Forman, G. J. Piermarini, J. D. Barnett, S. Block, *Science* **176**, 284 (1972).
14. See for example E. D. Jones, S. T. Tozer, and T. Schmiedel, *Physica E* **2**, 146 (1997).
15. R. L. Greene and K. K. Bajaj, *Phys. Rev. B* **31**, 913 (1985).
16. R. L. Greene and K. K. Bajaj, *Phys. Rev. B* **31**, 6498 (1985).